ASTRONOMY & ASTROPHYSICS
SUPPLEMENT SERIES

Astron. Astrophys. Suppl. Ser. **123,** 575-580 (1997)

Atomic data from the IRON Project

XXIII. Relativistic excitation rate coefficients for Fe XXII with inclusion of radiation damping⋆

H.L. Zhang and A.K. Pradhan

Department of Astronomy, The Ohio State University, Columbus, OH 43210, U.S.A.
Internet: zhang@payne.mps.ohio-state.edu

Received September 25; accepted October 8, 1996

Abstract. New collision strengths have been calculated for 990 transitions among 45 fine structure $n = 2$ and $n = 3$ levels of Fe XXII. The relativistic Breit-Pauli formulation of the R-matrix method was employed in the close coupling approximation, with radiation damping of autoionizing resonances included for the first time in the calculations of excitation rate coefficients. It is found that, at low temperatures, the relativistic effects considerably enhance rate coefficients for the intercombination transitions, and the radiation damping effect reduces those for a few transitions. It is also found that resonances due to coupling with the $n = 3$ levels significantly enhance rate coefficients for the transitions to low-lying levels at intermediate and high temperatures, and for the transitions to the $n = 2$ high-lying levels at all temperatures. It is expected that the new data, tabulated at a wide range of temperatures, would lead to a revision of the spectral diagnostics of Fe XXII in laboratory and astrophysical sources, in particular the X-ray spectra observed from solar flares and tokamaks.

Key words: atomic data — Sun: flares — X-rays: general

1. Introduction

Atomic data for highly charged B-like ions is of considerable interest in the study and modeling of high temperature astrophysical and laboratory plasmas. The spectra from ions in the Boron isoelectronic sequence are observed from a variety of astrophysical objects such as novae, planetary nebulae, Seyfert galaxies, the interstellar medium and the Sun. The spectral lines provide valuable temperature, density and abundance diagnostics in the wavelength range from the IR to the EUV. Of particular interest is the theoretical atomic data for Fe XXII for spectral lines in the EUV likely to be observed from the Solar and Heliospheric Observatory (SOHO) and the Extreme Ultraviolet Explorer (EUVE). Accurate atomic collision data for Fe XXII is also needed in the laboratory plasma diagnostics, particularly tokamaks.

Among highly charged B-like ions, Fe XXII deserves a more careful examination for the following reasons. (1) The relativistic effects, which give rise to fine-structure level splitting and intermediate-coupling type of mixing, are very important and should not be neglected; (2) resonances and the coupling effects are very pronounced and affect the rate coefficients for some transitions considerably (not only resonances due to the $n = 2$ levels but also the $n = 3$ levels, especially for the transitions to the high-lying $n = 2$ levels); and (3) autoionizing resonances may be subject to radiation damping which has not heretofore been taken into account in the calculation of excitation rates.

Many workers have calculated collision strengths and rate coefficients for Fe XXII, mostly in the distorted-wave approximation (see the data review for B-like ions by Sampson et al. 1994). There are also recent fully relativistic distorted-wave (RDW) results by Zhang & Sampson (1994a,b), which did not include the coupling and resonance effects. In a previous work, we have also calculated collision strengths and rate coefficients for the 105 transitions between the $n = 2$ levels in several Boron-like ions, including Fe XXII, published in Paper III of the present series (Zhang et al. 1994). The calculations were done using the R-matrix close-coupling method, with fine structure and the relativistic effects included rather approximately via an algebraic transformation of the scattering matrices using the relativistic term-coupling-coefficients (TCC) for the target ion (Eissner et al. 1974). However,

Send offprint requests to: H.L. Zhang

⋆ Table 3, 4 and 5 for complete data for Fe XXII are only available in electronic form at the CDS via anonymous ftp to cdsarc.u-strasbg.fr (130.79.128.5) or via http://cdsweb.u-strasbg.fr/Abstract.html

as pointed out by Zhang & Pradhan (1995a) and further demonstrated in Sect. 3, for highly charged ions such as Fe XXII, the TCC approach is not an adequate approximation to the relativistic effects, and furthermore, the radiation damping effect could be important for some transitions. Also, the target expansion in Paper III did not include $n = 3$ levels for the Fe XXII calculation, so that the resonances arising from coupling with these levels were omitted. Therefore, the results in that work for Fe XXII may not be accurate. In the present work, we employed the relativistic Breit-Pauli (BP) R-matrix method, which treats the intermediate coupling effects ab initio, to calculate electron-impact excitation collision strengths and rate coefficients for Fe XXII, using a 45 level target expansion. Radiation damping of autoionizing resonances using the Bell & Seaton (1985) theory of dielectronic recombination was included, and its effect on the rate coefficients was studied. To our knowledge, this is the first time that all three kinds of effects, 1) the relativistic effects, 2) the resonance and coupling effects and 3) the radiation damping effect, have been included simultaneously in an ab initio calculation of electron-impact excitation rate coefficients for positively charged ions.

The present calculation includes 15 $n = 2$ fine-structure levels and 30 $n = 3$ levels, as given in detail by Table 1. The Coulomb-Bethe approximation was employed to include the high partial-wave contributions for the optically allowed transitions. Collision strengths and maxwellian-averaged rate coefficients have been calculated for the 105 transitions among the 15 fine-structure levels of $n = 2$ configurations, the 450 transitions between these 15 $n = 2$ levels and the 30 $n = 3$ levels, and the 435 transitions among the 30 $n = 3$ levels. As in Paper III, rate coefficients are tabulated for scaled electron temperatures between 100 and 50 000 z^2 K, where the ion charge $z = Z - N$ with Z and N being the atomic number of the ion and the number of the electrons per ion. For Fe XXII, this corresponds to a range of T(K) from about 44 000 to 2.2 10^7. A brief description of the computations and the results are given in the following sections.

The present work is part of an international collaboration known as the IRON Project (Hummer et al. 1993, referred to as Paper I) to obtain accurate electron-impact excitation rates for fine-structure transitions in atomic ions. A full list of the papers in this Atomic Data from the IRON Project series published to-date is given in the references. A complete list of papers including those in press can be found at http://www.am.qub.uk/projects/iron/papers/, where abstracts are also given for each paper.

2. Atomic calculations

The method of calculating electron-impact excitation collision strengths using the BP R-matrix approximation is described in detail in Paper I of this series (Hummer et al. 1993) and in Berrington et al. (1995). Basically the Hamiltonian of the (e + ion) system includes the relativistic terms, that is the mass-velocity term, the Darwin term and the spin-orbit interaction. Consequently, the energy term of the target ion is split into fine-structure levels specified by the total angular momentum J_t and the parity π. An intermediate coupling representation is used in which J_t is coupled to the free-electron orbital angular momentum l and spin s in the following way:

$$\boldsymbol{J}_t + \boldsymbol{l} = \boldsymbol{K}, \quad \boldsymbol{K} + \boldsymbol{s} = \boldsymbol{J} \tag{1}$$

where K is an intermediate quantum number.

The target wavefunctions used in this calculation for Fe XXII are similar to those in Paper III, but with some improvements. Fifteen fine-structure energy levels dominated by $2s^22p$, $2s2p^2$ and $2p^3$ configurations and thirty $n = 3$ levels of the $2s^23s$, $2s^23p$, $2s^23d$, 2s2p3s and 2s2p3p configurations are included. The energy levels of the configurations 2s2p3d, $2p^23s$, $2p^23p$ and $2p^23d$ were not included since the present 45-state calculation was already computationally very demanding. We note that this will not significantly affect the results for transitions to the $n = 2$ levels. Table 1 lists the 45 levels and provides the key to the level indices used in tabulating the maxwellian-averaged collision strengths. The observed energies (Sugar & Corliss 1985) for all 15 $n = 2$ levels and 6 available $n = 3$ levels and the energies calculated here for all 45 levels are listed in Table 1 for comparison.

For collisional calculations, we include 24 total (e + ion) $J\pi$ symmetries with $0 \leq J \leq 11$ for both even and odd parities. These should provide convergence of the partial wave contributions for the forbidden transitions, and the low energy part of the intercombination and the optically allowed transitions. At energies greater than the highest $n = 2$ threshold ($E = 14.833$ Ryd), the higher partial waves for optically allowed transitions are calculated in the Coulomb-Bethe approximation, as in most of our electron-impact excitation work (see for example, Paper III).

As is well known, coupling and resonance effects may be important in the electron-impact excitation collision strengths for some highly charged ions, as is the case for Fe XXII. In the present calculation we have included these effects, not only those due to the $n = 2$ levels, but also those arising from the $n = 3$ levels, with a rather large fine-structure target expansion. We have used a quantum-defect mesh of free-electron energies (see Paper III for more detail), with a maximum effective quantum number $\nu_{\max}$ which defines the so-called "QDT" (quatum defect theory) region within which we consider radiation damping of resonances, i.e. for $\nu_{\max} \leq \nu \leq \infty$. In order to avoid unnecessary computations where this effect is not important, we take $\nu_{\max} = 45$ for electron energies E in the range zero to the highest $n = 2$ threshold ($E = 14.833$ Ryd), and $\nu_{\max} = 25$ for E further up to 79 Ryd. With the quantum-defect mesh, when $\nu \leq \nu_{\max}$, that

is when electron energies approach each excitation threshold but less than $E_{\rm th} - z^2/\nu_{\rm max}^2$ ($E_{\rm th}$ being the threshold energy), detailed resonance structures are resolved. When $\nu > \nu_{\rm max}$, resonance averaged values are obtained (Gailitis averaging - see Paper III) for energies up to the threshold. In all, collision strengths were calculated for more than 10 000 energy points. We calculated collision strengths for 79 Ryd $< E \leq 500$ Ryd using a coarser energy mesh since resonances are not important in this range.

The relativistic effects, which we included through the BP approximation in an ab initio manner, affect collision strengths mostly in two ways: 1) the energy splitting of a term into levels produces more complex resonance structures, and 2) the background collision strengths are affected through intermediate coupling of fine-structure levels for some transitions, mainly for the intercombination transitions.

As pointed out in Zhang & Pradhan (1995a), for highly charged ions, resonances may be subject to radiation damping. We include radiation damping by using the Bell-Seaton theory (Bell & Seaton 1985) of dielectronic recombination. As seen from Zhang & Pradhan (1995a), the radiation effect increases with the effective quantum number ν of the autoionizing states: it is negligible when the ν's are small, less than 10 in the present case. We calculated detailed collision strengths with radiation damping, using Eq. (3) in Zhang & Pradhan (1995a), for $10 \leq \nu \leq 45$, and the averaged collision strengths with radiation damping using Eq. (4) for $\nu > 45$ (the Gailitis averaging or QDT region). This was done for the resonances associated with the $n = 2$ levels of the target ion.

3. Results

In this section we present relativistic BP results for the maxwellian averaged collision strength, Υ, with radiation damping included. The effects of relativity and radiation damping on the maxwellian averaged collision strengths are examined.

The maxwellian averaged collision strength, or the effective collision strength, is given by:

$$\Upsilon_{ij} = \int_0^\infty \Omega_{ij} {\rm e}^{-\epsilon_j/kT} {\rm d}(\epsilon_j/kT), \qquad (2)$$

where Ω_{ij} is the collision strength for excitation from level i to level j, averaged over a maxwellian distribution of outgoing electron energies ϵ_j above the excitation threshold of the level j, at temperature T. This slowly varying function of temperature can then be used to obtain the rate coefficient, q_{ij}, for electron impact excitation,

$$q_{ij} = \frac{8.63\ 10^{-6}}{\sqrt{T} g_i} {\rm e}^{-E_{ij}/kT} \Upsilon_{ij} \qquad ({\rm cm}^3/{\rm s}) \qquad (3)$$

where E_{ij} is the energy difference between levels i and j and g_i is the statistical weight of level i.

The Υ values for the 105 transitions between the 15 $n = 2$ levels (see Table 1), the 450 transitions from these 15 $n = 2$ levels to the 30 $n = 3$ levels and the 435 transitions between these 30 $n = 3$ levels are tabulated for the same 32 z-scaled temperatures as those for the B-like ions in Paper III. We also calculated a set of results for the 105 transitions between the 15 $n = 2$ levels using a 15-level BP target expansion (15BP). In order to show the physical effects mentioned above, we compare in Table 2 the Υ results for 2 temperatures, $T = 441\ 000$ and 2 205 000 K, obtained with the 45-level target expansion (45BP), the 15BP, and the TCC calculations with the 8-term target (that corresponds to the same 15 levels as in 15BP) for transitions from the ground level 2p $^2{\rm P}^\circ_{1/2}$ to the fourteen excited $n = 2$ levels. The two sets of BP results for excitation to the low-lying levels are larger than those with the TCC (those for the lower temperature enhanced more), indicating the effect of the more extensive resonances due to relativistic level splitting in the BP calculations. For the intercombination transitions to the 2s2p^2 $^4{\rm P_J}$ levels (indices 3, 4 and 5 in the tables), the results with the BP are considerably larger than those with the TCC, obviously due to the relativistic intermediate coupling. For transitions to the high-lying $n = 2$ levels, namely the 2p^3 levels (indices 11 to 15 in the tables), the values for 45BP are generally higher than the 15BP, especially for the higher temperature $T = 2\ 205\ 000$ K, indicating the effect of resonances due to the $n = 3$ levels.

To further illustrate these effects, in Fig. 1 we compare the Υ values from the 45BP, 15BP, TCC and RDW (Zhang & Sampson 1994a) calculations for transitions from the ground level to the 2p $^2{\rm P}^\circ_{3/2}$, and the three 2s2p^2 $^4{\rm P_J}$ levels. It is seen that the values do not differ very much between the 15BP, the TCC and the RDW for the higher temperatures. The 45BP results are mostly higher than the three other sets at these temperatures, indicating the effect of the $n = 3$ resonances. For lower temperatures, the two sets of BP results are the same. However, they differ significantly from the TCC and the RDW results, especially for the intercombination transitions, showing that the relativistic effects affect the low-energy resonances. Obviously the RDW results are too low due to absence of resonance contributions. The TCC results are also low as explained by Fig. 1 of Zhang & Pradhan (1995a). From that figure we see that the TCC method takes relativistic effects into account only when the electron energies are greater than the target thresholds coupled to the upper level of the transition through intermediate mixing, while the BP method, in contrast, includes the relativistic effects ab initio for the entire energy region. Here it is again shown that the TCC method is not an adequate approximation for the relativistic effects in highly charged ions.

To study the radiation damping effect on the rate coefficients, we have also calculated the Υ values with this effect turned off. By examining the two sets of results, it

Table 1. Labeling of energy levels included in the calculation and the comparison of the observed and calculated energies (in rydbergs) in Fe XXII

i	Level	Observed	Theory	i	Level	Observed	Theory
1	$2s^22p\ ^2P^\circ_{1/2}$	0.00000	0.00000	24	$2s2p(^3P)3s\ ^2P^\circ_{1/2}$		78.37193
2	$2s^22p\ ^2P^\circ_{3/2}$	1.07776	1.05629	25	$2s2p(^3P)3p\ ^4D_{1/2}$		78.83664
3	$2s2p^2\ ^4P_{1/2}$	3.68653	3.63439	26	$2s2p(^3P)3p\ ^4D_{3/2}$		79.07484
4	$2s2p^2\ ^4P_{3/2}$	4.19365	4.13075	27	$2s2p(^3P)3s\ ^2P^\circ_{3/2}$		79.11491
5	$2s2p^2\ ^4P_{5/2}$	4.67717	4.64059	28	$2s2p(^3P)3p\ ^4D_{5/2}$		79.52481
6	$2s2p^2\ ^2D_{3/2}$	6.71166	6.73858	29	$2s2p(^3P)3p\ ^2P_{1/2}$	78.22317	79.52855
7	$2s2p^2\ ^2D_{5/2}$	6.92217	6.94497	30	$2s2p(^3P)3p\ ^2P_{3/2}$	79.17089	79.41152
8	$2s2p^2\ ^2P_{1/2}$	7.77748	7.82265	31	$2s2p(^3P)3p\ ^4P_{1/2}$		79.79154
9	$2s2p^2\ ^2S_{1/2}$	8.91420	8.93489	32	$2s2p(^3P)3p\ ^2D_{3/2}$	79.64474	79.90941
10	$2s2p^2\ ^2P_{3/2}$	9.04241	9.09880	33	$2s2p(^3P)3p\ ^4D_{7/2}$		80.16203
11	$2p^3\ ^4S^\circ_{3/2}$	11.44278	11.43474	34	$2s2p(^3P)3p\ ^4P_{3/2}$		80.27484
12	$2p^3\ ^2D^\circ_{3/2}$	12.72512	12.77092	35	$2s2p(^3P)3p\ ^4S_{3/2}$		80.39784
13	$2p^3\ ^2D^\circ_{5/2}$	13.00269	13.07500	36	$2s2p(^3P)3p\ ^4P_{5/2}$		80.44491
14	$2p^3\ ^2P^\circ_{1/2}$	14.30352	14.37056	37	$2s2p(^3P)3p\ ^2D_{5/2}$	80.60158	80.87084
15	$2p^3\ ^2P^\circ_{3/2}$	14.83288	14.88660	38	$2s2p(^3P)3p\ ^2S_{1/2}$		81.14805
16	$2s^23s\ ^2S_{1/2}$		74.08994	39	$2s2p(^1P)3s\ ^2P^\circ_{1/2}$		81.18313
17	$2s^23p\ ^2P^\circ_{1/2}$		75.74732	40	$2s2p(^1P)3s\ ^2P^\circ_{3/2}$		81.21893
18	$2s^23p\ ^2P^\circ_{3/2}$		76.01977	41	$2s2p(^1P)3p\ ^2P_{1/2}$		82.82656
19	$2s2p(^3P)3s\ ^4P^\circ_{1/2}$		77.41721	42	$2s2p(^1P)3p\ ^2D_{3/2}$		82.83533
20	$2s^23d\ ^2D_{3/2}$	77.43948	77.57156	43	$2s2p(^1P)3p\ ^2D_{5/2}$		83.03150
21	$2s^23d\ ^2D_{5/2}$	77.52149	77.65898	44	$2s2p(^1P)3p\ ^2P_{3/2}$		83.11559
22	$2s2p(^3P)3s\ ^4P^\circ_{3/2}$		77.69215	45	$2s2p(^1P)3p\ ^2S_{1/2}$		83.47909
23	$2s2p(^3P)3s\ ^4P^\circ_{5/2}$		78.31381				

Table 2. Comparison of the effective collision strengths Υ obtained from the relativistic Breit Pauli R-matrix method with the 45 level target expansion (45 BP) and with the 15 level expansion (15 BP), and by the term coupling method with the 8 term (15 level) target expansion (TCC) for Fe XXII. All three sets of the results include radiation damping effect

	$T = 441000$			$T = 2205000$		
j	45 BP	15 BP	TCC	45 BP	15 BP	TCC
2	1.51E-01	1.51E-01	1.40E-01	8.89E-02	8.20E-02	8.02E-02
3	1.23E-02	1.21E-02	6.12E-03	1.18E-02	9.47E-03	9.35E-03
4	1.31E-02	1.31E-02	7.67E-03	9.00E-03	7.46E-03	5.93E-03
5	1.29E-02	1.29E-02	6.42E-03	7.99E-03	6.92E-03	5.19E-03
6	1.97E-01	1.79E-01	1.59E-01	2.52E-01	2.59E-01	2.14E-01
7	1.09E-02	1.09E-02	1.96E-02	6.31E-03	5.39E-03	7.54E-03
8	2.44E-01	2.27E-01	2.29E-01	2.92E-01	3.04E-01	2.91E-01
9	1.10E-02	8.69E-03	6.71E-03	1.33E-02	1.16E-02	8.65E-03
10	5.20E-02	4.47E-02	4.41E-02	5.99E-02	5.98E-02	5.54E-02
11	3.34E-04	4.74E-04	2.98E-04	4.38E-04	4.03E-04	3.21E-04
12	9.89E-04	9.88E-04	1.07E-03	1.19E-03	9.94E-04	1.13E-03
13	5.70E-04	5.33E-04	7.51E-04	7.38E-04	5.25E-04	6.55E-04
14	7.71E-04	4.51E-04	8.99E-04	9.36E-04	4.84E-04	9.39E-04
15	1.13E-04	9.23E-05	1.07E-04	2.80E-04	9.15E-05	1.08E-04

is found that, although radiation damping affects collision strengths near a few target thresholds for some transitions, especially for the forbidden and the intercombination transitions, the effect on the rate coefficients is minimal for most transitions, only reducing the results by 1% or 2%, except for three transitions, $2p\ ^2P^\circ_{1/2} - 2p\ ^2P^\circ_{3/2}$, $2p\ ^2P^\circ_{1/2} - 2s2p^2\ ^2D_{5/2}$ and $2p\ ^2P^\circ_{3/2} - 2s2p^2\ ^2D_{3/2}$. For these three transitions, not only is the radiation damping effect on the collision strengths large, but its contribution to the rate coefficient is enhanced since the scattered electron energies, which enter the exponential term in Eq. (1), are small near the next target threshold where radiation damping is most pronounced. In Fig. 2 comparisons of the BP Υ values with and without radiation damping are made for four transitions, including the above three transitions and the transition $2p\ ^2P^\circ_{1/2} - 2s2p^2\ ^4P_{5/2}$. For the former three transitions the radiation damping effect reduces the Υ values by about $8 - 20\%$ at low temperatures,

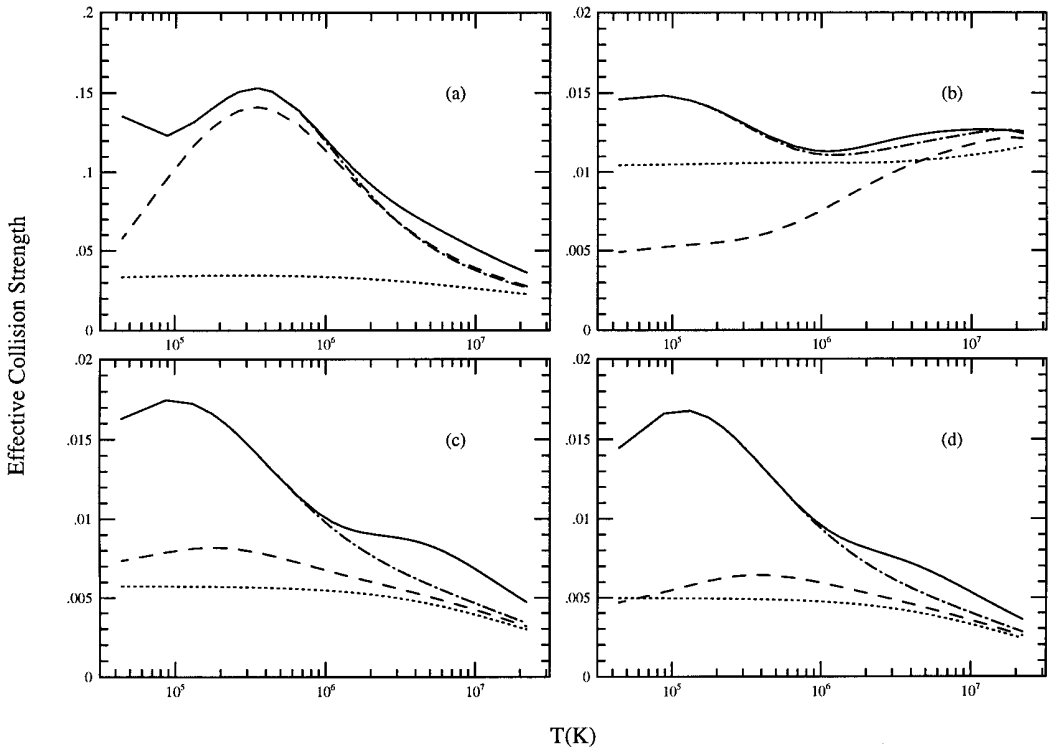

Fig. 1. Comparison of the present effective collision strengths by the relativistic Breit-Pauli R-matrix method with the 45-level target (the solid lines) and the 15-level target (the dash-dotted lines), by the term-coupling method (the dashed lines) and by the relativistic distorted-wave method (the dotted lines) for the transitions from the ground level $2s^2 2p\ ^2P^\circ_{1/2}$ to **a)** $2s^2 2p\ ^2P^\circ_{3/2}$, **b)** $2s2p^2\ ^4P_{1/2}$, **c)** $2s2p^2\ ^4P_{3/2}$ and **d)** $2s2p^2\ ^4P_{5/2}$

but for the latter transition the reduction is just about 2% (although its effect on the collision strength can be seen in Fig. 2 of Zhang & Pradhan 1995a).

The Υ values for the 105 $\Delta n = 0$ transitions, with $n = 2$, are tabulated in Table 3 at 32 z-scaled temperatures (T in z^2 K, so that actual T values are obtained by multiplying by $z^2 = 441$). Results for the 450 $n = 2 - 3$ transitions and for the 435 $\Delta n = 0$ transitions with $n = 3$ are tabulated in Table 4 and Table 5, respectively. Tables 3, 4 and 5 are not reproduced here, but are available in electronic form at the CDS, or via ftp from the authors at zhang@payne.mps.ohio-state.edu.

4. Discussion

In this section we give an estimate of the accuracy of our tabulated data.

In the present calculations for Fe XXII, all known important physical effects are included for electron-impact excitation collision strengths for highly charged ions with moderately high nuclear charge Z. These are resonance and coupling effects, relativistic effects, and radiation damping of resonances. Therefore, we expect these results to be rather accurate.

For the transitions between the $n = 2$ levels, since all the above effects were taken into account, the collision strengths and consequently the rate coefficients should be accurate to approximately $10 - 30\%$. We expect the accuracy of the transitions to the low-lying levels and of optically allowed transitions to be better than 20%. For the transitions from the $n = 2$ to the $n = 3$ levels, for which the resonances play a minor role but coupling to the $2s2p3d$, $2p^2 3s$, $2p^2 3p$ and $2p^2 3d$ states was neglected, the uncertainties in the rate coefficients could be higher, $30 - 50\%$. For the transitions between the $n = 3$ levels the uncertainties could possibly be more than $30 - 50\%$ for the same reason, and perhaps because of higher partial wave contributions than included here.

Acknowledgements. We would like to thank Dr. Werner Eissner for his assistance in the calculation and Dr. David Hummer, the coordinator of the IRON Project, for his comments. This work was supported by a grant (PHY-9421898) from the U.S. National Science Foundation. The computational work was carried out on the Cray Y-MP8/64 and the massively parallel Cray T3D at the Ohio Supercomputer Center in Columbus, Ohio.

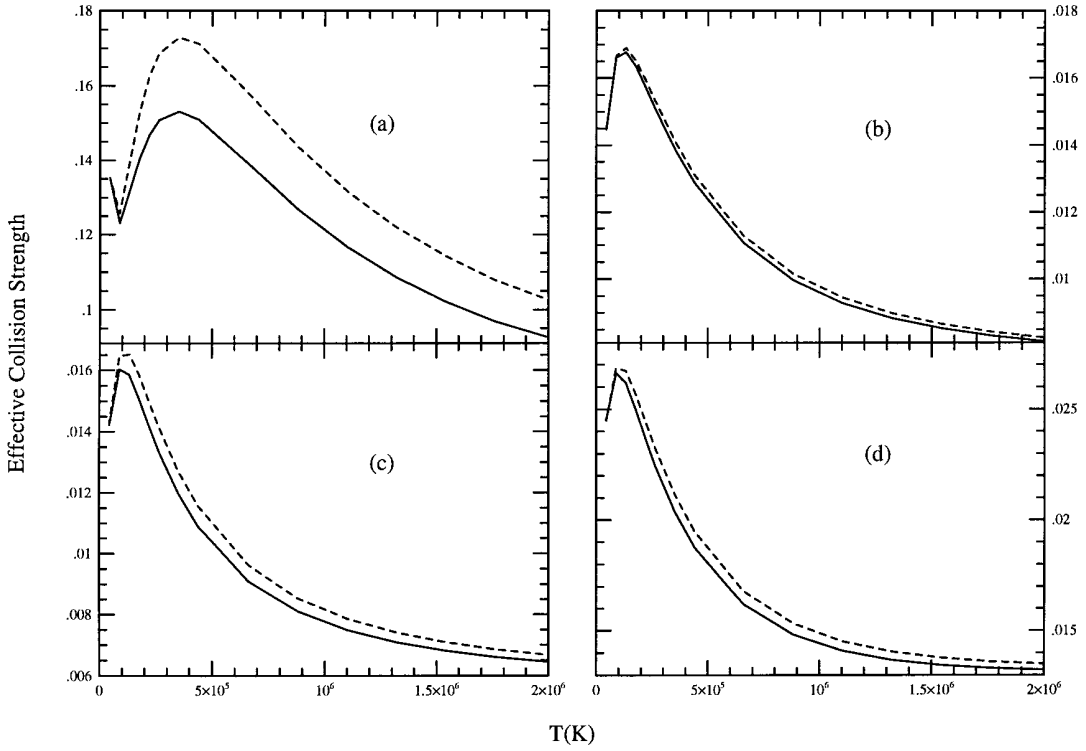

Fig. 2. Radiation damping effects on the effective collision strengths for the transitions **a)** $2s^2 2p\ ^2P^\circ_{1/2} - 2s^2 2p\ ^2P^\circ_{3/2}$, **b)** $2s^2 2p\ ^2P^\circ_{1/2} - 2s2p^2\ ^4P_{5/2}$, **c)** $2s^2 2p\ ^2P^\circ_{1/2} - 2s2p^2\ ^2D_{5/2}$ and **d)** $2s^2 2p\ ^2P^\circ_{3/2} - 2s2p^2\ ^2D_{3/2}$. The solid lines indicate the results with radiation damping and the dashed line those without radiation damping

References

Bautista M.A., Pradhan A.K., 1996, A&AS 115, 551 (Paper XIII)

Bautista M.A., 1996, A&AS 119, 105 (Paper XVI)

Bautista M.A., 1997, A&AS 122, 167 (Paper XX)

Bell R.H., Seaton M.J., 1985, J. Phys. B 18, 1589

Berrington K.A., 1995, A&AS 109, 193 (Paper VIII)

Berrington K.A., Eissner W.B., Norrington P.H., 1995, Comp. Phys. Comm. 92, 290

Berrington K.A., Pelan J.C., 1995, A&AS 114, 367 (Paper XII)

Butler K., Zeippen C.J., 1994, A&AS 108, 1 (Paper V)

Eissner W., Jones M., Nussbaumer H., 1974, Comp. Phys. Comm. 8, 270

Galavis M.E., Mendoza C., Zeippen C.J., 1995, A&AS 111, 347 (Paper X)

Hummer D.G., Berrington K.A., Eissner W., Pradhan A.K, Saraph H.E., Tully J.A., 1993, A&A 279, 298 (Paper I)

Kisielius R., Berrington K.A., Norrington P.H., 1996, A&AS 118, 157 (Paper XV)

Lennon D.J., Burke V.M., 1994, A&AS 103, 273 (Paper II)

Nahar S.N., 1995, A&A 293, 967 (Paper VII)

Nahar S.N., Pradhan A.K., 1996, A&AS 119, 509 (Paper XVII)

Pelan J., Berrington K.A., 1995, A&AS 110, 209 (Paper IX)

Quinet P., Le Dourneuf M., Zeippen C.J., 1997, A&AS 120, 361 (Paper XIX)

Sampson D.H., Zhang H.L., Fontes C.J., 1994, Atom. Data Nucl. Data Tab. 57, 97

Saraph H.E., Storey P.J., 1996, A&AS 115, 151 (Paper XI)

Saraph H.E., Tully J.A., 1994, A&AS 107, 29 (Paper IV)

Storey P.J., Mason H.E., Saraph H.E., 1996, A&A 309, 677 (Paper XIV)

Sugar J., Corliss C., 1985, J. Phys. Chem. Ref. Data 14, Suppl. 2

Zhang H.L., 1996, A&AS 119, 523 (Paper XVIII)

Zhang H.L., Graziani M., Pradhan A.K., 1994, A&A 283, 319 (Paper III)

Zhang H.L., Pradhan A.K., 1995a, J. Phys. B 28, L285

Zhang H.L., Pradhan A.K., 1995b, A&A 293, 953 (Paper VI)

Zhang H.L., Sampson D.H., 1994a, Atom. Data Nucl. Data Tab. 56, 41

Zhang H.L., Sampson D.H., 1994b, Atom. Data Nucl. Data Tab. 58, 255